

## WING PITCHING MOMENT AT ZERO LIFT AT SUBCRITICAL MACH NUMBERS

### 1. NOTATION AND UNITS

		<i>SI</i>	<i>British</i>
$A$	aspect ratio, $b/\bar{c}$		
$b$	wing span	m	ft
$C_{LLT}$	local lift coefficient due to effective twist		
$C_{m0}$	pitching moment coefficient at zero total wing lift, $M_0^{1/2}\rho V^2 S \bar{c}$		
$(C_{m0})_1$	contribution to $C_{m0}$ due to $(C_{m0})_\infty$ , modified for planform effects		
$(C_{m0})_2$	contribution to $C_{m0}$ due to effective twist		
$c$	local chord	m	ft
$c_r$	wing root (centre-line) chord	m	ft
$c_t$	wing tip chord	m	ft
$\bar{c}$	standard (geometric) mean chord, $\int_0^1 c d\eta$	m	ft
$\bar{\bar{c}}$	aerodynamic mean chord, $\int_0^1 (c^2/\bar{c}) d\eta$	m	ft
$F$	empirical correction factor applied to $(C_{m0i})_{\infty th}$		
$f$	empirical correction factor in Equation (3.9) for $(C_{m0i})_1$		
$g$	function of taper ratio in Equation (3.24)		
$h$	function of aspect ratio and sweepback in Equation (3.25)		
$k$	empirical factor in Equation (3.21)		
$M$	free-stream Mach number		
$M_0$	pitching moment at zero total wing lift, positive nose up	N m	lbf ft
$S$	wing planform area, $b\bar{c}$	$m^2$	$ft^2$
$V$	free-stream velocity	m/s	ft/s
$x$	streamwise co-ordinate, positive aft	m	ft

$x_{1/4}$	streamwise location of local quarter-chord point referred to leading edge of wing root chord	m	ft
$\bar{x}$	streamwise location of $1/4 \bar{c}$ referred to leading edge of wing root chord, see Sketch 3.1	m	ft
$z_c$	camber ordinate	m	ft
$\alpha_0$	angle of attack at zero lift	degree	degree
$\beta$	compressibility parameter, $(1 - M^2)^{1/2}$		
$\delta$	local geometric twist (angle of local chord relative to root chord, positive leading edge up)	degree	degree
$\delta_c$	local camber-dependent twist in Equation (3.17)	degree	degree
$\delta_e$	effective wing twist, $\delta + \delta_c$ , see Equation (3.18)	degree	degree
$\delta_{et}$	value of $\delta_e$ at tip	degree	degree
$\delta'_{et}$	equivalent linear tip twist, see Equation (3.28)	degree	degree
$\eta$	spanwise distance from root as fraction of semi-span		
$\bar{\eta}$	spanwise location of $\bar{c}$ , see Sketch 3.1		
$\eta_n$	$\cos (n\pi/8)$		
$\Lambda_{1/4}$	sweepback of $1/4$ -chord line	degree	degree
$\Lambda_{1/2}$	sweepback of mid-chord line	degree	degree
$\lambda$	taper ratio, $c_t/c_r$		
$\rho$	free-stream air density	kg/m <sup>3</sup>	slug/ft <sup>3</sup>

### Subscripts

<i>expt</i>	denotes experimental value
<i>i</i>	denotes incompressible flow
<i>pred</i>	denotes predicted value
<i>r</i>	denotes value at wing root
<i>t</i>	denotes value at wing tip
<i>th</i>	denotes approximate theoretical value
0	denotes zero total wing lift

- $\infty$  denotes wing sectional value in two-dimensional flow
- $\eta$  denotes value at spanwise location  $\eta$
- $\eta_n$  denotes value at  $\eta_n$  ( $n = 1, 2, 3$ ), see section 3.3.2

A bar (–) over a symbol denotes an average value.

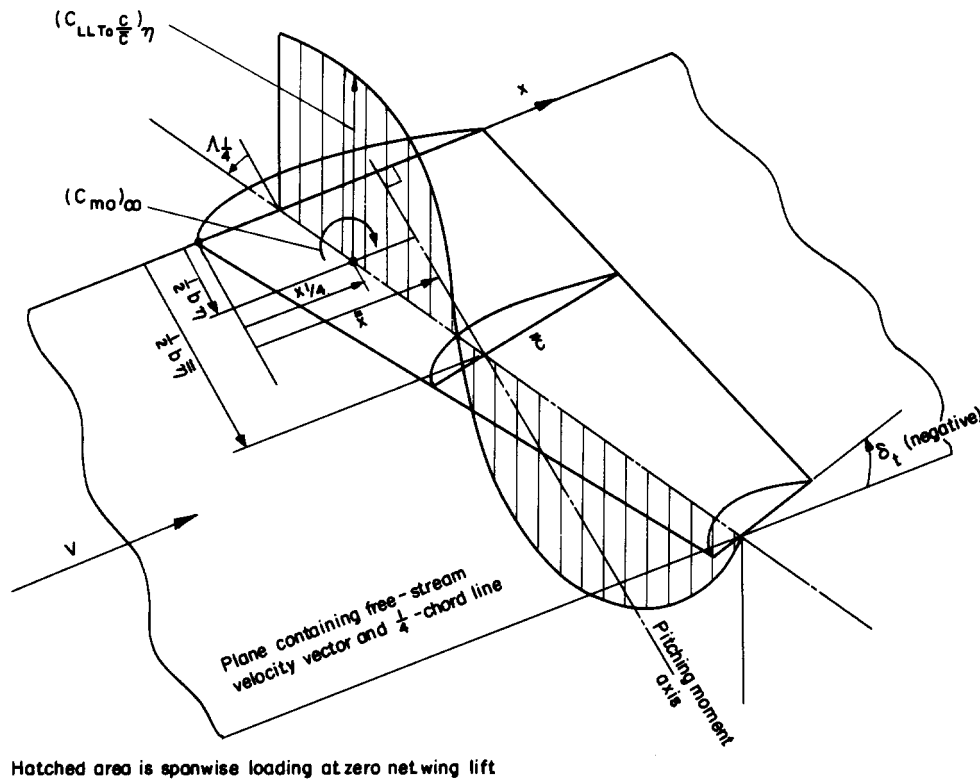
## 2. INTRODUCTION

This Item provides a simple semi-empirical method for estimating wing pitching moment coefficient at zero lift at subcritical Mach numbers. The method, presented in Section 3, consists of separate estimations of the low-speed contributions due to the overall effect of camber via sectional pitching moments at zero lift and due to the combined effects of geometric and camber-dependent twist, modified for the effect of Mach number in the subcritical range. The contribution due to the overall effects of camber via sectional pitching moment at zero lift (Section 3.2) is based on an approximate theoretical estimate for the wing sectional profile, corrected by means of empirical factors for the approximations involved in the theoretical estimate and for planform effects. The contribution due to the combined effects of geometric and camber-dependent twist (Section 3.3) is based on strip theory using the theoretical spanwise loading due to twist. Two forms of the method are given, a simple one for application in those cases in which the twist distribution is linear and a more general one for those cases in which the twist distribution is highly non-linear. Also given is a simpler alternative method, which is satisfactory for most cases of non-linear twist, in which the method for linear twist is employed in conjunction with an equivalent linear twist. The effect of Mach number is given in Section 3.4.

The applicability and accuracy of the method are discussed in Section 4 and an illustration of a typical use of the Item is given in worked examples in Section 6. Appendix A provides details of a computer program, available on diskette in the Aerodynamics Software Volume.

## 3. WING ZERO-LIFT PITCHING MOMENT

### 3.1 General



**Sketch 3.1 Cambered and twisted wing at zero lift**

From Sketch 3.1 it can be seen that in the most general case of a cambered and twisted swept wing the wing pitching moment coefficient at zero lift can be considered to consist of two contributions. The first contribution,  $(C_{m0})_1$ , arises from the integration across the span of local (sectional) values,  $(C_{m0})_{\infty}$ , of  $C_{m0}$ , modified for planform effects. The second contribution,  $(C_{m0})_2$ , adds the effect of twist through another spanwise integration involving  $C_{LLT0} c/\bar{c}$ , the load distribution at zero total wing lift. The load distribution at zero total wing lift arises from a combination of geometric twist and what can be termed “camber-dependent” twist for those cases in which the camber line, and hence the local zero-lift angle of attack, varies across the span. The zero-lift pitching moment coefficient can therefore be written as

$$C_{m0} = (C_{m0})_1 + (C_{m0})_2 \quad (3.1)$$

where,

$$(C_{m0})_1 = f(A, \Lambda_{1/2}) \int_0^1 \frac{(C_{m0})_{\infty} c^2}{\bar{c}} d\eta \quad (3.2)$$

and

$$(C_{m0})_2 = \int_0^1 \frac{\bar{x} - x_{1/4}}{\bar{c}} \left( C_{LLT0} \frac{c}{\bar{c}} \right)_{\eta} d\eta. \quad (3.3)$$

The practical evaluation of Equations (3.2) and (3.3) for low speeds is given in Sections 3.2 and 3.3 respectively. The effect of Mach number is considered in Section 3.4.

### 3.2 Evaluation of $(C_{m0i})_1$

From Equation (3.2) the contribution  $(C_{m0i})_1$  is given by

$$(C_{m0i})_1 = f(A, \Lambda_{1/2}) \int_0^1 \frac{(C_{m0i})_\infty c^2}{\bar{c} \frac{c}{\bar{c}}} d\eta \quad (3.4)$$

$$= f(A, \Lambda_{1/2}) (\bar{C}_{m0i})_\infty \quad (3.5)$$

where  $(\bar{C}_{m0i})_\infty$  incorporates any effects of wing taper and is a spanwise average of the local two-dimensional values

$$(C_{m0i})_\infty = F(C_{m0i})_{\infty th} \quad (3.6)$$

Here,  $(C_{m0i})_{\infty th}$  is the value obtained by using Item No. 72024 (Derivation 3), and the empirical correction factor  $F$ , in Figure 1, is a function of  $(C_{m0i})_{\infty th}$  obtained from comparisons of  $(C_{m0i})_{\infty th}$  with wind-tunnel test data for a large number of aerofoils in Derivations 1, 2 and 4 to 12. If the camber line is unchanged across the wing span then  $(C_{m0i})_{\infty th}$  is constant, giving

$$(\bar{C}_{m0i})_\infty = F(C_{m0i})_{\infty th} \quad (3.7)$$

*i.e.* independent of wing taper. If, however, the camber line varies across the span a good approximation to  $(\bar{C}_{m0i})_\infty$  for straight tapered wings is given by

$$(\bar{C}_{m0i})_\infty = \frac{3}{2(1 + \lambda + \lambda^2)} \left\{ [F(C_{m0i})_{\infty th}]_{0.2} (0.8 + 0.2\lambda)^2 + [F(C_{m0i})_{\infty th}]_{0.8} (0.2 + 0.8\lambda)^2 \right\} \quad (3.8)$$

which is based on the integrand of Equation (3.4) at the carefully chosen spanwise locations  $\eta = 0.2$  and  $0.8$ .

The empirical factor,  $f(A, \Lambda_{1/2})$ , correcting for planform effects in Equation (3.4) was found from an analysis of wind-tunnel data on wings (Derivations 14 to 30) to be given by

$$f(A, \Lambda_{1/2}) = \frac{2A}{2A + 1} \cos \Lambda_{1/2} \quad (3.9)$$

Equation (3.4) therefore becomes, in the most general case,

$$(C_{m0i})_1 = \frac{3A \cos \Lambda_{1/2}}{(2A + 1)(1 + \lambda + \lambda^2)} \left\{ [F(C_{m0i})_{\infty th}]_{0.2} (0.8 + 0.2\lambda)^2 + [F(C_{m0i})_{\infty th}]_{0.8} (0.2 + 0.8\lambda)^2 \right\} \quad (3.10)$$

which, within a good approximation, reduces to

$$(C_{m0i})_1 = \frac{2A}{2A + 1} \cos \Lambda_{1/2} F(C_{m0i})_{\infty th} \quad (3.11)$$

when the camber line is unchanged across the span.

### 3.3 Evaluation of $(C_{m0i})_2$

From Equation (3.3) the contribution  $(C_{m0i})_2$  is given by

$$(C_{m0i})_2 = \int_0^1 \frac{(\bar{x} - x_{1/4})}{\bar{c}} \left( C_{LLT0} \frac{c}{\bar{c}} \right)_\eta d\eta. \quad (3.12)$$

From Sketch 3.1 for a straight tapered wing

$$\frac{(\bar{x} - x_{1/4})}{\bar{c}} = \frac{b}{2\bar{c}} (\bar{\eta} - \eta) \tan \Lambda_{1/4} = \frac{A}{2} (\bar{\eta} - \eta) = \frac{\bar{c}}{c} \tan \Lambda_{1/4} \quad (3.13)$$

where 
$$\frac{\bar{c}}{c} = \frac{3(1 + \lambda)^2}{4(1 + \lambda + \lambda^2)} \quad (3.14)$$

and\* 
$$\bar{\eta} = \frac{1}{3} \left( \frac{1 + 2\lambda}{1 + \lambda} \right). \quad (3.15)$$

Equation (3.12) therefore becomes,

$$(C_{m0i})_2 = \frac{3(1 + \lambda)^2}{8(1 + \lambda + \lambda^2)} A \tan \Lambda_{1/4} \int_0^1 (\bar{\eta} - \eta) \left( C_{LLT0i} \frac{\bar{c}}{c} \right)_\eta d\eta, \quad (3.16)$$

where  $\bar{\eta}$  is given by Equation (3.15). In Equation (3.16)  $(C_{LLT0i} c/\bar{c})_\eta$  is the local loading at zero total wing lift due to the combined effects of local geometric twist,  $\delta$ , and local camber-dependent twist,  $\delta_c$ . The local geometric twist is defined as the angle of the local chord relative to the root (centre-line) chord, and the local camber-dependent twist is defined as the difference between local and root section values of  $\alpha_{0i}$ , *i.e.*

$$\delta_c = (\alpha_{0ir})_\infty - (\alpha_{0i})_\infty. \quad (3.17)$$

Thus a combined, or effective, local twist,  $\delta_e$ , can be given as

$$\delta_e = \delta + \delta_c = \delta + (\alpha_{0ir})_\infty - (\alpha_{0i\eta})_\infty \quad (3.18)$$

which can be interpreted as the angle of the local zero-lift line relative to that of the root section. An estimate of  $(\alpha_{0i\eta})_\infty$  can be obtained from Item No. 87031 (Derivation 45).

At the tip, Equation (3.18) becomes

$$\delta_{et} = \delta_t + (\alpha_{0ir})_\infty - (\alpha_{0it})_\infty. \quad (3.19)$$

When the camber line is unchanged across the span,  $(\alpha_{0ir})_\infty = (\alpha_{0it})_\infty$ , and Equation (3.19) reduces to

$$\delta_{et} = \delta_t. \quad (3.20)$$

\* Note that in Item No. 83040 (Reference 47)  $\bar{\eta}$  is given the symbol  $\kappa$ .

### 3.3.1 Linear twist

Analysis of approximate solutions to Equation (3.16), in Derivation 34, for wings with a linear spanwise distribution of twist, has shown that the integral in that equation can be approximated by

$$\int_0^1 (\bar{\eta} - \eta) \left( C_{LLT0i} \frac{c}{c} \right)_{\eta} d\eta \approx -k \bar{\eta} \frac{A}{A + 10} \delta_{et} \quad (3.21)$$

for  $2 \leq A \leq 10$  and  $0 \leq A \tan \Lambda_{1/4} \leq 6$  where

$$k = 0.019 \text{ for } 0 \leq \lambda \leq 0.5$$

falling to  $k = 0.017$  for  $\lambda = 1$ .

When Equations (3.15) and (3.21) are substituted into it, Equation (3.16) becomes

$$\boxed{\frac{(C_{m0i})_2}{\delta_{et}} = -\frac{k(1+\lambda)(1+2\lambda)}{8(1+\lambda+\lambda^2)} \frac{A^2}{(A+10)} \tan \Lambda_{1/4}} \quad (3.22)$$

with the planform restrictions and values of  $k$  as set out below Equation (3.21).

Equation (3.22) can be written as

$$\frac{(C_{m0i})_2}{\delta_{et}} = g(\lambda) h(A, A \tan \Lambda_{1/4}) \quad (3.23)$$

$$\text{where } g(\lambda) = \frac{k(1+\lambda)(1+2\lambda)}{8(1+\lambda+\lambda^2)} \quad (3.24)$$

$$\text{and } h(A, A \tan \Lambda_{1/4}) = -\frac{A}{A+10} A \tan \Lambda_{1/4}. \quad (3.25)$$

Equations (3.24) and (3.25) are presented graphically in Figures 2 and 3.

Provided that the spanwise distribution of effective twist is linear Equation (3.22) would be expected to provide satisfactory estimates. For effective twist distributions that are highly non-linear a different approach is required.

### 3.3.2 Non-linear twist

For wings with a general distribution of effective twist, Derivation 34 gives

$$\boxed{(C_{m0i})_2 = -\frac{3}{8} \frac{(1+\lambda)^2}{(1+\lambda+\lambda^2)} A \tan \Lambda_{1/4} \left[ 0.126 \left( C_{LLT0i} \frac{c}{c} \right)_{\eta_1} + 0.175 \left( C_{LLT0i} \frac{c}{c} \right)_{\eta_2} + 0.106 \left( C_{LLT0i} \frac{c}{c} \right)_{\eta_3} \right]} \quad (3.26)$$

where  $(C_{LLT0i}c/\bar{c})_{\eta}$  is the spanwise loading at zero total lift due to given values of effective twist,  $\delta_e$ , at  $\eta = \eta_n = \cos(n\pi/8)$  with  $\eta_1 = 0.924$ ,  $\eta_2 = 0.707$  and  $\eta_3 = 0.383$ . The spanwise loading can be obtained from the approximate method of Item No. 83040 (Reference 47). However, the use of Equation (3.26), even with the simple method of Item No. 83040 is somewhat time consuming and it has been found that the use of an equivalent linear twist  $\delta'_{et}$  dependent on values of  $\delta_e$  at  $\eta = 0.2$  and  $0.8$  in conjunction with Equation (3.22) gives satisfactory agreement with values obtained using the full procedure of Equation (3.26). Thus, even for some cases of extreme discontinuous twist distribution, such as those used in Examples 8.1 and 8.3 of Item No. 83040, it is sufficient to take

$$(C_{m0i})_2 = -\frac{k(1+\lambda)(1+2\lambda)}{8(1+\lambda+\lambda^2)} \frac{A^2}{A+10} \delta'_{et} \tan \Lambda_{1/2} \quad (3.27)$$

where the equivalent linear twist is given by

$$\delta'_{et} = (\delta_{e,0.8} - \delta_{e,0.2})/0.6 \quad (3.28)$$

and, from Equation (3.18),

$$\delta_{e,0.2} = \delta_{0.2} + (\alpha_{0ir})_{\infty} - (\alpha_{0i,0.2})_{\infty} \quad (3.29)$$

$$\delta_{e,0.8} = \delta_{0.8} + (\alpha_{0ir})_{\infty} - (\alpha_{0i,0.8})_{\infty} \quad (3.30)$$

### 3.4 Effect of Mach Number

From simple considerations of the effect of compressibility on  $(C_{m0i})$ , the contributions  $(C_{m0})_1$  and  $(C_{m0})_2$  are given by

$$(C_{m0})_1 = \frac{2A+1}{2\beta A+1} (C_{m0i})_1 \quad (3.31)$$

and

$$(C_{m0})_2 = \frac{A+10}{\beta A+10} (C_{m0i})_2 \quad (3.32)$$

in which  $\beta = (1-M^2)^{1/2}$  and  $(C_{m0i})_1$  and  $(C_{m0i})_2$  are obtained respectively from Equations (3.10) or (3.11) and (3.22), (3.26) or (3.27).

## 4. APPLICABILITY AND ACCURACY

The method given in this Item for estimating wing pitching moment coefficient at zero lift at subcritical Mach numbers is applicable to straight tapered wings with camber and twist provided that the local effective twist is not excessive ( $\delta_e \leq 10$  degrees, say) and provided that the flow over the wing is attached and wholly subsonic at the zero-lift condition. The method has been applied successfully to wings with cranked or curved edges by means of the "equivalent wing planform" concept detailed in Item No. 76003 (Reference 46).

The method can cope (via Derivation 3) with any shape of camber line which can also vary across the span. In principle, the method is capable of dealing with any form of spanwise twist distribution but is simplest to use for wings with an approximately linear twist distribution. For most applications of non-linear twist the use of an equivalent linear twist in conjunction with the simple linear twist method is found to be satisfactory.

It is recommended that use of the method be restricted in general to planforms in the ranges  $\lambda \leq 1$ ,  $2 \leq A \leq 10$  and  $0 \leq A \tan \Lambda_{1/4} \leq 6$ . For untwisted wings the upper limit on aspect ratio can be exceeded and moreover the method can be applied to wings with forward sweep.

The method has been compared with wind-tunnel test data for a wide range of aerofoils (Derivations 1, 2 and 4 to 12) and wings both without geometric twist (Derivations 14 to 30) and with twist (Derivations 17, 18, 21, 27, 31 to 33 and 35 to 44). The comparisons for low-speed flow are shown in Sketches 4.1 to 4.3 for aerofoils, unswept wings and swept wings, respectively. The test data correlate to within about  $\pm 15$  per cent for those cases inside the previously stated limitations on planform and twist. However, for  $|C_{m0i}| \leq 0.02$  correlation to within about  $\pm 0.005$  can be expected. The effects of fixing boundary-layer transition and of varying the Reynolds number (provided that it is greater than about  $10^6$  based on  $\bar{c}$ ) can be ignored within these error bands.

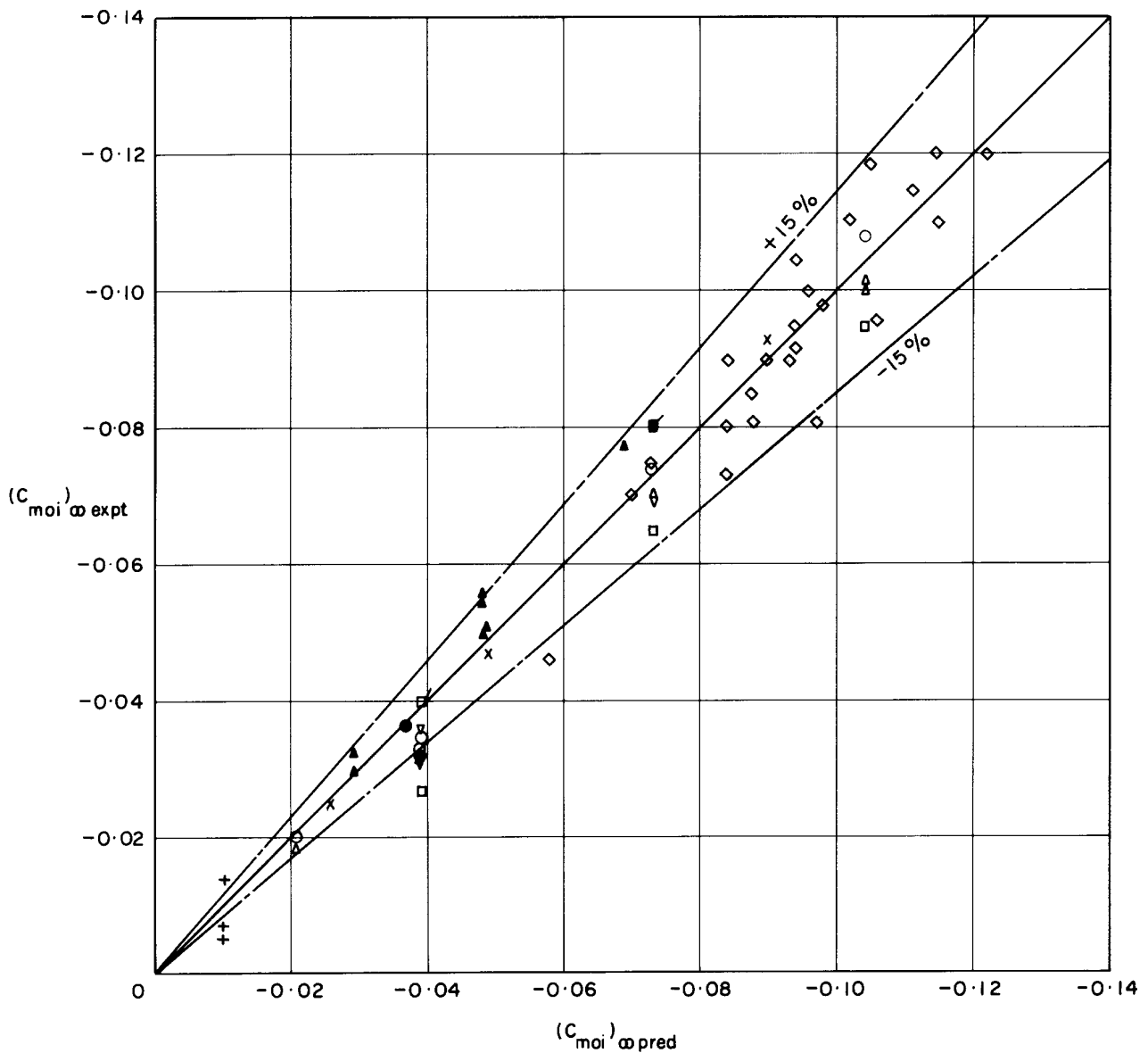
The effect of compressibility for both aerofoils and wings using Equations (3.1), (3.31) and (3.32) has been compared with wind-tunnel test data from Derivations 13, 20, 21, 22, 26, 35, 43 and 44. For subcritical Mach numbers the accuracy of the method is in general unchanged from that at low speeds.

Most of the test data were restricted to straight-tapered swept-back wings; exceptionally, Derivations 19 and 22 related to swept-forward wings without twist and Derivations 29 and 30 related to a wing with cranked trailing edges.

### Conventional NACA aerofoils

Symbol	Family	NACA mean line
x	NACA 4-digit	64
+	NACA 5-digit	230
o	NACA 63	$\alpha = 1$
□	NACA 64	$\alpha = 1$
△	NACA 65	$\alpha = 1$
▽	NACA 66	$\alpha = 1$
●	NACA 63	$\alpha = 0.3$
▲	NACA 65	$\alpha = 0.5, 0.6, 0.8$
▼	NACA 66	$\alpha = 0.6$
♂	NACA 63A	$\alpha = 0.8$ (mod)
♂	NACA 64A	$\alpha = 0.8$ (mod)

◇ Modern aerofoils

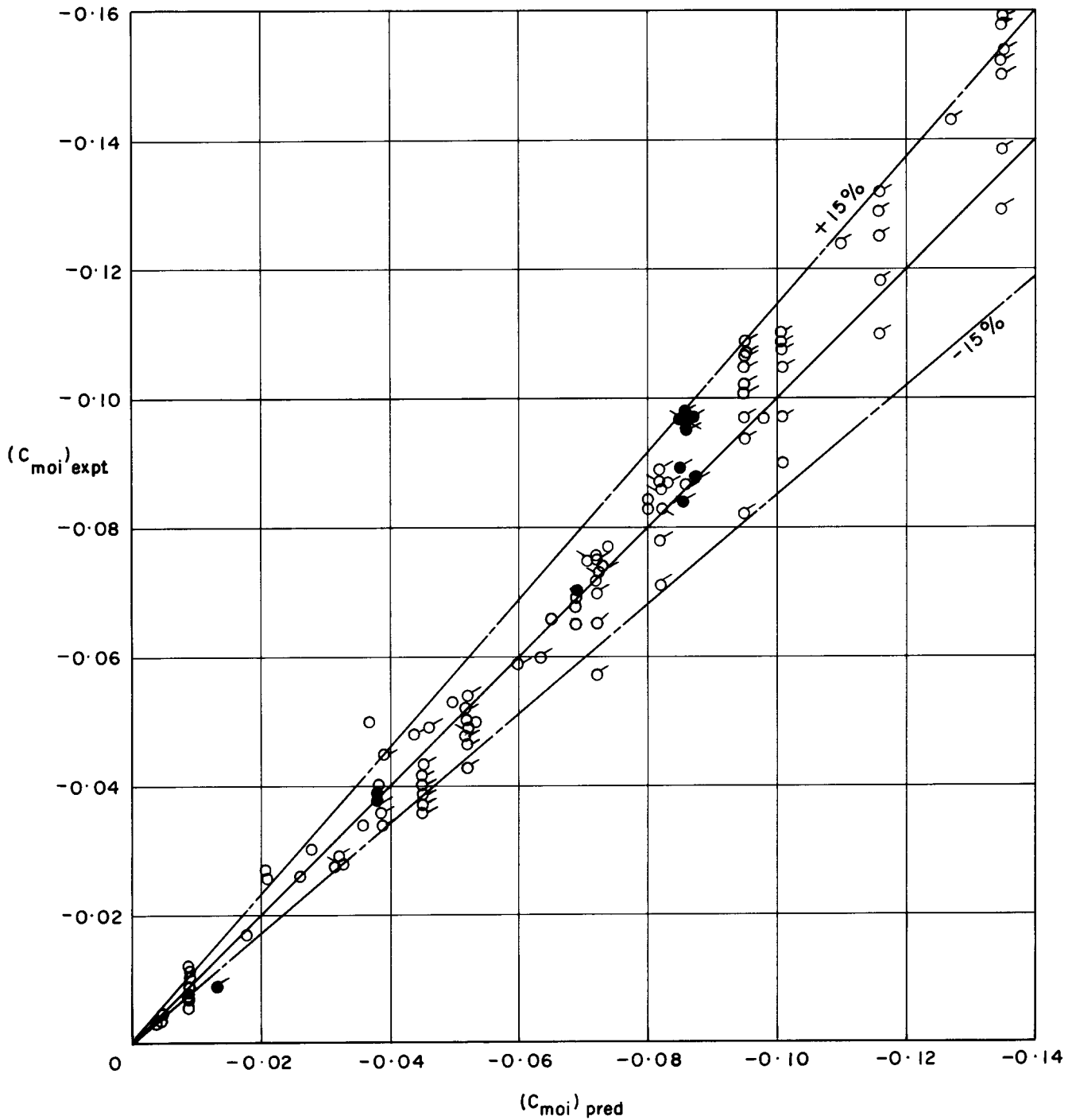


Sketch 4.1 Correlation of method with test data for aerofoils

○ Without twist

● With twist

Prime (') denotes wing with NACA 4-digit section

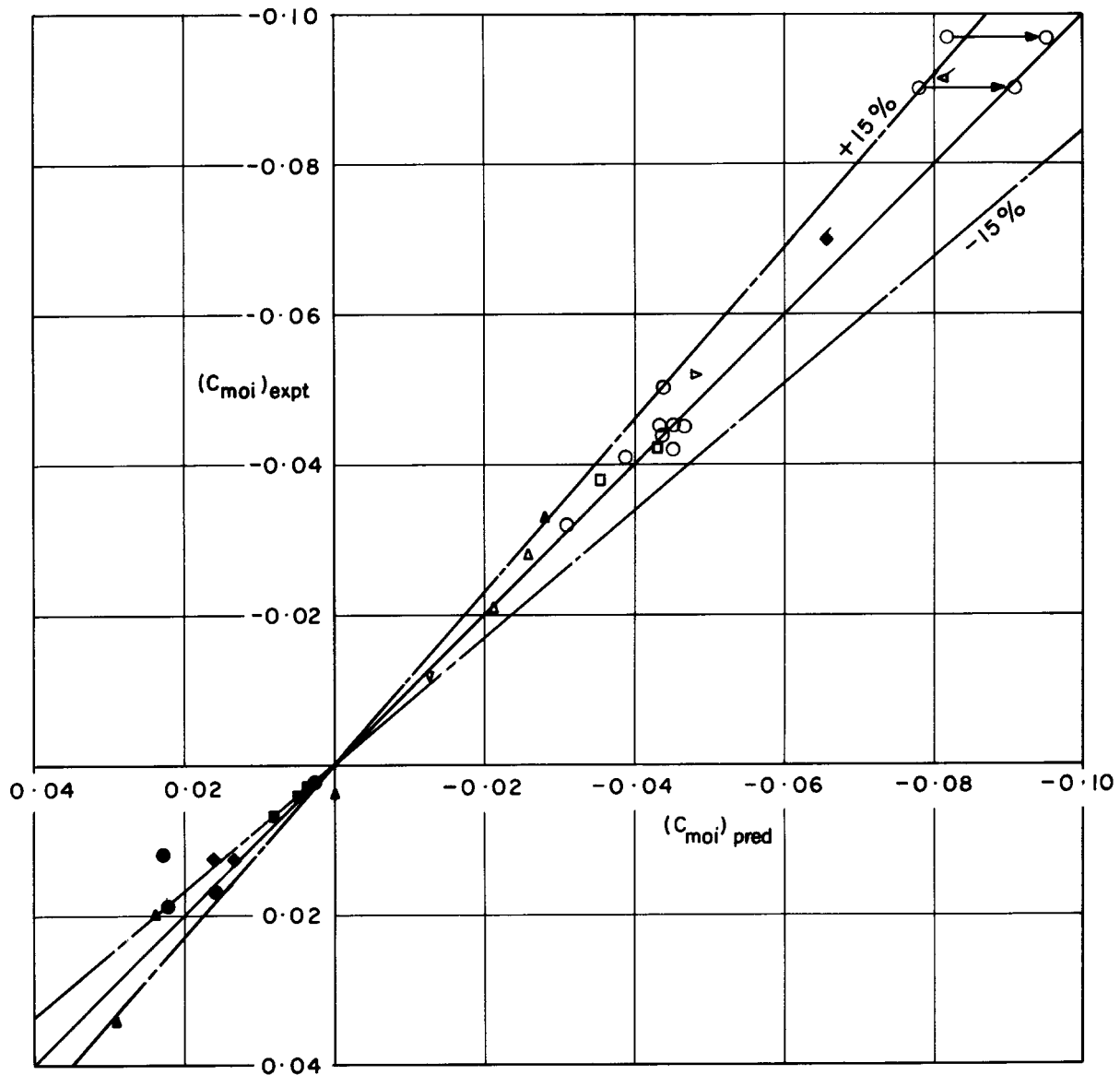


Sketch 4.2 Correlation of method with test data for unswept wings ( $\Lambda_{1/4} = 0$ )

	$\Lambda_{1/4}$
▽	- 46
◄	- 12
■	15
◆	22 to 23
●	28 to 40
▲	45 to 46
▷	61

Note:

- (i) Open symbols represent wings with no twist
- (ii) Filled symbols represent wings with twist  
( $-3.5 \leq \delta_t \leq -8.5$ )
- (iii) Primed (') symbols denote wings with NACA 4-digit sections
- (iv)  $\longrightarrow$  denotes improvement using test data for  $(C_{moi})_\infty$



Sketch 4.3 Correlation of method with test data for swept wings  $\Lambda_{1/4} \neq 0$

## 5. DERIVATION AND REFERENCES

### 5.1 Derivation

The Derivation lists selected sources that have assisted in the preparation of this Item.

#### Aerofoils

1. LOFTIN, L.K. Theoretical and experimental data for a number of NACA 6A-series airfoil sections. NACA Report 903, 1948.
2. ABBOTT, I.H. THEORY OF WING SECTIONS. Published by Dover Publications Inc., New York, 1959.
3. ESDU Aerodynamic characteristics of aerofoils in compressible inviscid airflow at subcritical Mach numbers. Item No. 72024. ESDU International plc, London, 1972.
4. McGHEE, R.J. BEASLEY, W.D. Low speed aerodynamic characteristics of a 17-percent-thick airfoil section designed for general aviation applications. NASA tech. Note D-7428, 1973.
5. McGHEE, R.J. BEASLEY, W.D. Effect of thickness on the aerodynamic characteristics of an initial low-speed family of airfoils for general aviation applications. NASA tech. Memor. 72843, 1976.
6. McGHEE, R.J. BEASLEY, W.D. Low speed wind tunnel results for a modified 13-percent-thick airfoil. NASA tech. Memor.-X 74018, 1979.
7. McGHEE, R.J. BEASLEY, W.D. Wind tunnel results for an improved 21-percent-thick low-speed airfoil section. NASA tech. Memor. 78650, 1978.
8. ALTHAUS, D. WORTMANN, F.X. STUTTGARTER PROFILKATALOG I. Published by F. Vieweg and Son, Braunschweig/Wiesbaden, 1979.
9. McGHEE, R.J. BEASLEY, W.D. Low speed aerodynamic characteristics of a 13-percent-thick medium speed airfoil designed for general aviation applications. NASA tech. Paper 1498, 1979.
10. HARRIS, C.D. BEASLEY, W.D. Low speed aerodynamic characteristics of a 14-percent-thick NASA phase 2 supercritical airfoil designed for a lift coefficient of 0.7. NASA tech. Memor. 81912, 1980.
11. McGHEE, R.J. BEASLEY, W.D. Low speed aerodynamic characteristics of a 17-percent-thick medium speed airfoil designed for general aviation applications. NASA tech. Paper 1786, 1980.
12. McGHEE, R.J. BEASLEY, W.D. Wind tunnel results for a modified 17-percent-thick low-speed airfoil section. NASA tech. Paper 1919, 1981.
13. ARA Unpublished work at Aircraft Research Association, Bedford.

#### Wings with Camber

14. ANDERSON, R.F. The aerodynamic characteristics of airfoils at negative angles of attack. NACA tech. Note 412, 1932.

15. JACOBS, E.N.  
WARD, K.E.  
PINKERTON, R.M. The characteristics of 78 related airfoil sections from tests in the variable density wind tunnel. NACA Report 460, 1933.
16. JACOBS, E.N.  
CLAY, W.C. Characteristics of the NACA 23012 airfoil from tests in the full-scale and variable-density tunnels. NACA Report 530, 1935.
17. ANDERSON, R.F. Determination of the characteristics of tapered wings. NACA Report 572, 1936.
18. ANDERSON, R.F. The experimental and calculated characteristics of 22 tapered wings. NACA Report 627, 1938.
19. MENDELSON, R.A.  
BREWER, J.D. Comparison between the measured and theoretical span loading on a moderately swept-forward and a moderately swept-back semispan wing. NACA tech. Note 1351, 1946.
20. WHITCOMB, R.T. Investigation of the characteristics of a high-aspect-ratio-wing in the Langley 8-foot high-speed tunnel. NACA RM L6H28a (TIL 1138), 1946.
21. HAMILTON, W.T.  
NELSON, W.H. Summary report on the high speed characteristics of six model wings having NACA 65-series sections. NACA Report 877, 1947.
22. HIESER, G.  
WHITCOMB, C.F. Investigation of the effects of a nacelle on the aerodynamic characteristics of a swept wing and the effects of sweep on a wing alone. NACA tech. Note 1709, 1948.
23. HOPKINS, E.J. A wind-tunnel investigation at low speed of various lateral controls on a 45° swept-back wing. NACA RM A7L16 (TIL 1613), 1948.
24. ANSCOMBE, A.  
RANEY, D.J. Low speed tunnel investigation of the effect of the body on  $C_{mo}$  and aerodynamic centre of unswept wing-body combinations. ARC CP 16, 1950.
25. RILEY, D.R. Wind tunnel investigation and analysis of the effects of end plates on the aerodynamic characteristics of an unswept wing. NACA tech. Note 2440, 1951.
26. TINLING, B.E.  
KOLK, W.R. The effects of Mach number and Reynolds number on the aerodynamic characteristics of several 12-percent-thick wings having 35° of sweepback and various amounts of camber. NACA RM A50K27 (TIL 2629), 1951.
27. ROSE, L.M. Low-speed characteristics of a wing having 63° sweepback and uniform camber. NACA RM A51D25 (TIL 2781), 1951.
28. BREBNER, G.G.  
WYATT, L.A.  
ILOTT, G.P. Low speed wind tunnel tests on a series of rectangular wings of varying aspect ratio and aerofoil section. ARC CP 916, 1967.
29. KIRBY, D.A.  
HEPWORTH, A.G. Low speed wind-tunnel tests of the longitudinal stability characteristics of some swept-wing quiet airbus configurations. RAE tech. Rep. 76029, 1976.

30. LOVELL, D.A. A wind-tunnel investigation of the effects of flap span and deflection angle, wing planform and a body on the high-lift performance of a 28° swept wing. RAE tech. Rep. 76030, 1976.

#### Wings with Camber and Geometric Twist

31. CONNER, D.W. Effect of reflex camber on the aerodynamic characteristics of a highly tapered moderately swept-back wing at Reynolds numbers up to 8,000,000. NACA tech. Note 1212, 1946.
32. NEELY, R.H.  
BOLLECH, T.V.  
WESTRICK, G.C.  
GRAHAM, R.R. Experimental and calculated characteristics of several NACA 44-series wings with aspect ratios of 8, 10 and 12 and taper ratios of 2.5 and 3.5. NACA tech. Note 1270, 1947.
33. LETKO, W.  
FEIGENBAUM, D. Wind-tunnel investigation of split trailing-edge lift and trim flaps on a tapered wing with 23° sweepback. NACA tech. Note 1352, 1947.
34. DeYOUNG, J.  
HARPER, C.W. Theoretical symmetric span loading at subsonic speeds for wings having arbitrary planform. NACA Report 921, 1948.
35. WEST, F.E.  
HALLISSY, J.M. Effects of compressibility on normal-force, pressure, and load characteristics of a tapered wing of NACA 66-series airfoil sections with split flaps. NACA tech. Note 1759, 1948.
36. BOLLECH, T.V. Experimental and calculated characteristics of several high-aspect-ratio tapered wings incorporating NACA 44-series, 230-series and low-drag 64-series airfoil sections. NACA tech. Note 1677, 1948.
37. SIVELLS, J.C.  
SPOONER, S.H. Investigation in the Langley 19-foot pressure tunnel of two wings of NACA 65-210 and 64-210 airfoil sections with various type flaps. NACA Report 942, 1949.
38. TROUNCER, J.  
KETTLE, D. Low speed model tests on two “V” wings. ARC R & M 2364, 1950.
39. WEIBERG, J.A.  
CAREL, H.C. Wind-tunnel investigation at low speed of a wing swept back 63° and twisted and cambered for uniform load at a lift coefficient of 0.5 and with a thickened tip section. NACA RM A50I14 (TIL 2559), 1950.
40. JAQUET, B.M. Effect of linear spanwise variations of twist and circular-arc camber on low-speed static stability, rolling, and yawing characteristics of a 45° sweptback wing of aspect ratio 4 and taper ratio 0.6. NACA tech. Note 2775, 1952.
41. SALMI, R.J. Low-speed longitudinal aerodynamic characteristics of a twisted and cambered wing of 45° sweepback and aspect ratio 8 with and without high-lift and stall-control devices and a fuselage at Reynolds numbers from  $1.5 \times 10^6$  to  $4.8 \times 10^6$ . NACA RM L52C11 (TIL 3192), 1952.
42. PRATT, G.L. Effects of twist and camber on the low-speed longitudinal stability characteristics of a 45° sweptback wing of aspect ratio 8 at Reynolds numbers from  $1.5 \times 10^6$  to  $4.8 \times 10^6$  as determined by pressure distributions, force tests and calculations. NACA RM L52J03a (TIL 3541), 1952.
43. BOLTZ, F.W.  
KOLBE, C.D. The forces and pressure distribution at subsonic speeds on a cambered and twisted wing having 45° of sweepback, an aspect ratio of 3 and a taper ratio of 0.5. NACA RM A52D22 (TIL 3268), 1952.

44. EDWARDS, G.G.  
TINLING, B.E.  
ACKERMAN, A.C.      The longitudinal characteristics at Mach numbers up to 0.92 of a cambered and twisted wing having  $40^\circ$  of sweepback and an aspect ratio of 10. NACA RM A52F18 (TIL 3318), 1952.
45. ESDU      Wing angle of attack for zero lift at subcritical Mach numbers. Item No. 87031. ESDU International plc, London, 1987.

See also Derivations [17](#), [18](#), [21](#) and [27](#).

## 5.2 References

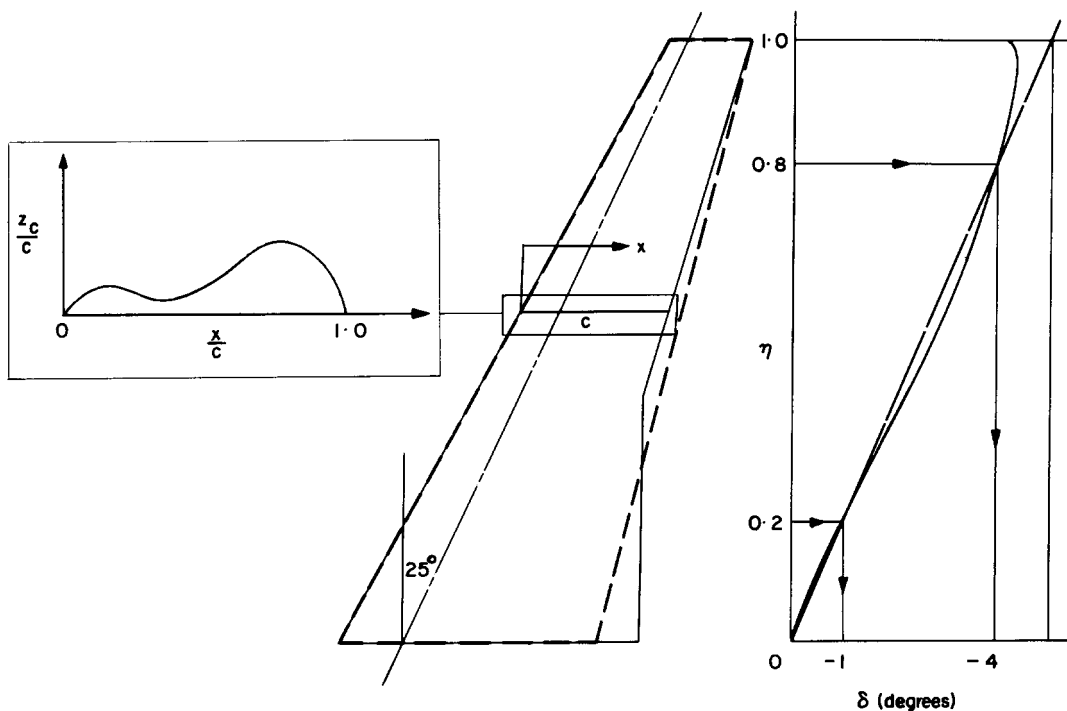
The References are sources of information supplementary to that given in this Item.

46. ESDU      Geometrical properties of cranked and straight tapered wing planforms. Item No. 76003. ESDU International plc, London, 1976.
47. ESDU      Method for the rapid estimation of spanwise loading of wings with camber and twist in subsonic attached flow. Item No. 83040. ESDU International plc, London, 1983.

## 6. EXAMPLES

### 6.1 Example 1

The pitching moment coefficient at zero lift and a Mach number of 0.8 is required for the wing shown in Sketch 6.1. The planform parameters for the equivalent wing, shown dotted, are  $A = 7$ ,  $\Lambda_{1/4} = 25^\circ$ ,  $\Lambda_{1/2} = 21.3^\circ$ , and  $\lambda = 0.3$ . The wing has a fixed section with the camber line ordinates in Table 6.1 shown in Sketch 6.2. The wing has a spanwise distribution of twist, shown in Sketch 6.3.



Sketch 6.2 Camber line

Sketch 6.1 Wing Planform

Sketch 6.3 Twist distribution

**TABLE 6.1 Camber line ordinates**

$x/c$	$z_c/c$	$x/c$	$z_c/c$
0	0	0.5	0.0047
0.025	0.0028	0.6	0.0082
0.050	0.0037	0.7	0.0104
0.1	0.0045	0.8	0.0105
0.2	0.0038	0.9	0.0079
0.3	0.0022	0.95	0.0050
0.4	0.0020	1.0	0

Use of Addendum A of Item No. 72024 (Derivation 3) gives, for the camber line ordinates in Table 6.1,

$$(C_{m0i})_{\infty th} = -0.0589.$$

From Figure 1, with this value,  $F = 0.87$ .

Equation (3.11) therefore gives, for  $A = 7$  and  $\Lambda_{1/2} = 21.3^\circ$ ,

$$\begin{aligned} (C_{m0i})_1 &= \frac{2A}{2A+1} \cos \Lambda_{1/2} F (C_{m0i})_{\infty th} \\ &= \frac{14}{15} \times 0.9317 \times 0.87 \times (-0.0589) \\ &= -0.0446. \end{aligned}$$

Equation (3.31) gives the effect of Mach number as

$$(C_{m0})_1 = \frac{2A+1}{2\beta A+1} (C_{m0i})_1$$

which, for  $M = 0.8$  (i.e.  $\beta = 0.6$ ),  $A = 7$  and  $(C_{m0i})_1 = -0.0446$ , gives

$$\begin{aligned} (C_{m0})_1 &= \frac{15}{9.4} \times (-0.0446) \\ &= 1.596 \times (-0.0446) = -0.0712. \end{aligned}$$

Equation (3.27) gives, for  $\lambda = 0.3$ ,  $A = 7$ ,  $\Lambda_{1/4} = 25^\circ$  and  $k = 0.019$ ,

$$\begin{aligned} (C_{m0i})_2 &= -\frac{k}{8} \frac{(1+\lambda)(1+2\lambda)}{(1+\lambda+\lambda^2)} \frac{A^2}{(A+10)} (\tan \Lambda_{1/4}) \delta'_{et} \\ &= -\frac{0.019}{8} \times \frac{1.3 \times 1.6}{1.39} \times \frac{49}{17} \times 0.4663 \times \delta'_{et} \\ &= -0.00478 \times \delta'_{et}. \end{aligned}$$

From Sketch 6.3 and Equation (3.28) the equivalent linear twist,  $\delta'_{et}$ , is given as

$$\delta'_{et} = [-4 - (-1)]/0.6 = -5^\circ.$$

Therefore

$$\begin{aligned}(C_{m0i})_2 &= (-0.00478) \times (-5) \\ &= 0.0239.\end{aligned}$$

Equation (3.32) gives the effect of Mach number as

$$(C_{m0})_2 = \frac{A + 10}{\beta A + 10} (C_{m0i})_2$$

which, for  $\beta = 0.6$ ,  $A = 7$  and  $(C_{m0i})_2 = 0.0239$  gives

$$\begin{aligned}(C_{m0})_2 &= \frac{17}{14.2} \times 0.0239 \\ &= 1.197 \times 0.0239 = 0.0286.\end{aligned}$$

Therefore, from Equation (3.1)

$$\begin{aligned}C_{m0} &= (C_{m0})_1 + (C_{m0})_2 \\ &= -0.0712 + 0.0286 \\ &= -0.0426.\end{aligned}$$

It can be seen that the nose-down pitch due to camber has been considerably alleviated by the application of twist to reduce the local angle of attack of the outboard sections compared with the root section (*i.e.* “wash-out”), the primary uses of which on swept-back wings are to prevent premature tip stalling and to produce a spanwise loading nearer to the elliptical ideal.

It is worth noting that  $C_{m0i} = -0.0446 + 0.0239 = -0.0207$ , which compares with  $C_{m0} = -0.0426$ , showing that in this example compressibility effects cause the zero-lift pitching moment to double its magnitude.

## 6.2 EXAMPLE 2

It is required to offset further the inherent nose-down pitching moment at zero lift for the wing of Example 1 by maintaining the camber line at the wing tip but reducing the camber ordinates linearly to zero at the wing root.

Because the camber line is now varying (linearly) across the span, Equation (3.10) is appropriate. In that equation values of  $F(C_{m0i})_{\infty th}$  at  $\eta = 0.2$  and  $0.8$  are required.

Because the camber ordinates are proportional to  $\eta$

$$[(C_{m0i})_{\infty th}]_{\eta} = \eta [(C_{m0i})_{\infty th}]_1$$

since  $C_{m0i} \propto z_c/c \propto \eta(z_c/c)_1$ .

Therefore  $[(C_{m0i})_{\infty th}]_{0.8} = 0.8 \times (-0.0589) = -0.0471$

and, from Figure 1, the corresponding  $F = 0.89$ .

Similarly,  $[(C_{m0i})_{\infty th}]_{0.2} = -0.118$  and  $F = 0.96$ .

Therefore, Equation (3.10) gives, with  $A = 7$ ,  $\Lambda_{1/2} = 21.3^\circ$  and  $\lambda = 0.3$ ,

$$\begin{aligned} (C_{m0i})_1 &= \frac{3A \cos \Lambda_{1/2}}{(2A + 1)(1 + \lambda + \lambda^2)} \left\{ [F(C_{m0i})_{\infty th}]_{0.2} (0.8 + 0.2\lambda)^2 \right. \\ &\quad \left. + [F(C_{m0i})_{\infty th}]_{0.8} (0.2 + 0.8\lambda)^2 \right\} \\ &= \frac{21 \times 0.9317}{15 \times 1.39} \{ 0.96(-0.0118)(0.86)^2 + 0.89(-0.0471)(0.44)^2 \} \\ &= -0.0155. \end{aligned}$$

which, with the compressibility factor of 1.597 obtained in Example 1, gives

$$(C_{m0})_1 = 1.597 \times (-0.0155) = -0.0248.$$

The change in camber distribution has therefore reduced the magnitude of  $(C_{m0})_1$  by 65 per cent. However, due to a reduction in the effective twist, this will be partially offset by a decrease in  $(C_{m0})_2$ , as follows.

Use of Item No. 87031 gives, for the camber line ordinates in Table 6.1,

$$(\alpha_{0ir})_{\infty} = -1.68 \text{ degrees, and given that } (\alpha_{0ir})_{\infty} = 0, \text{ therefore}$$

$$(\alpha_{0i, 0.8})_{\infty} = 0.8 \times (-1.68) = -1.344 \text{ degrees}$$

and  $(\alpha_{0i, 0.2})_{\infty} = 0.2 \times (-1.68) = -0.336 \text{ degrees}.$

Therefore, Equations (3.29) and (3.30) give

$$\begin{aligned} \delta_{e, 0.2} &= \delta_{0.2} + (\alpha_{0ir})_{\infty} - (\alpha_{0i, 0.2})_{\infty} \\ &= -1 + 0 - (-0.336) \\ &= -0.664 \text{ degrees.} \end{aligned}$$

and  $\delta_{e, 0.8} = \delta_{0.8} + (\alpha_{0ir})_{\infty} - (\alpha_{0i, 0.8})_{\infty}$

$$\begin{aligned} &= -4 + 0 - (-1.344) \\ &= -2.656 \text{ degrees.} \end{aligned}$$

Thus from Equation (3.28)

$$\begin{aligned}\delta'_{et} &= (\delta_{e, 0.8} - \delta_{e, 0.2})/0.6 \\ &= [-2.656 - (-0.664)]/0.6 \\ &= -1.992/0.6 = -3.32 \text{ degrees.}\end{aligned}$$

Therefore, with  $(C_{m0i})_2 = -0.00478 \times \delta'_{et}$  from Example 1,

$$\begin{aligned}(C_{m0i})_2 &= -0.00478 \times (-3.32) \\ &= 0.0159,\end{aligned}$$

*i.e.* a reduction of about 33 per cent which, with the compressibility factor of 1.197 obtained in Example 1, gives  $(C_{m0})_2 = 0.0190$ .

Thus, from Equation (3.1)

$$\begin{aligned}C_{m0} &= (C_{m0})_1 + (C_{m0})_2 \\ &= -0.0248 + 0.0190 \\ &= -0.0058.\end{aligned}$$

It can be seen that the particular combination of spanwise variation of camber and geometric twist has resulted in a wing with a very small pitching moment at zero lift.

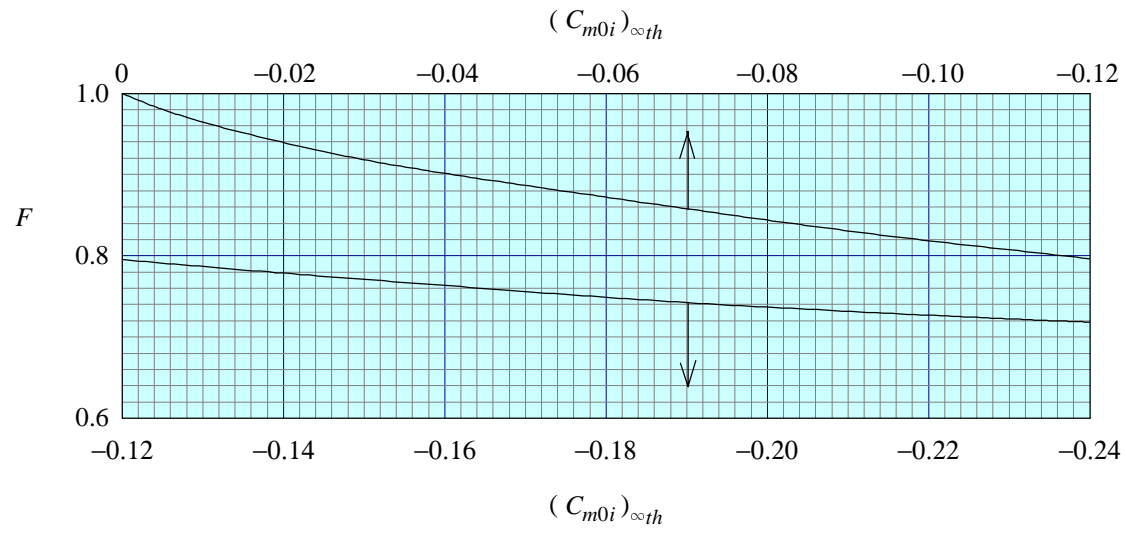


**FIGURE 1**

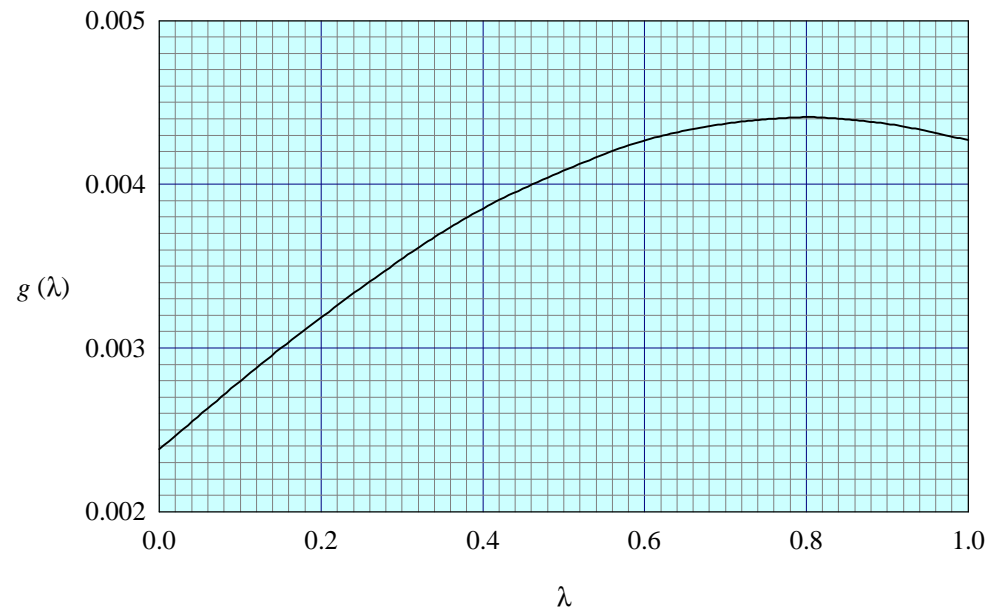


**FIGURE 2**

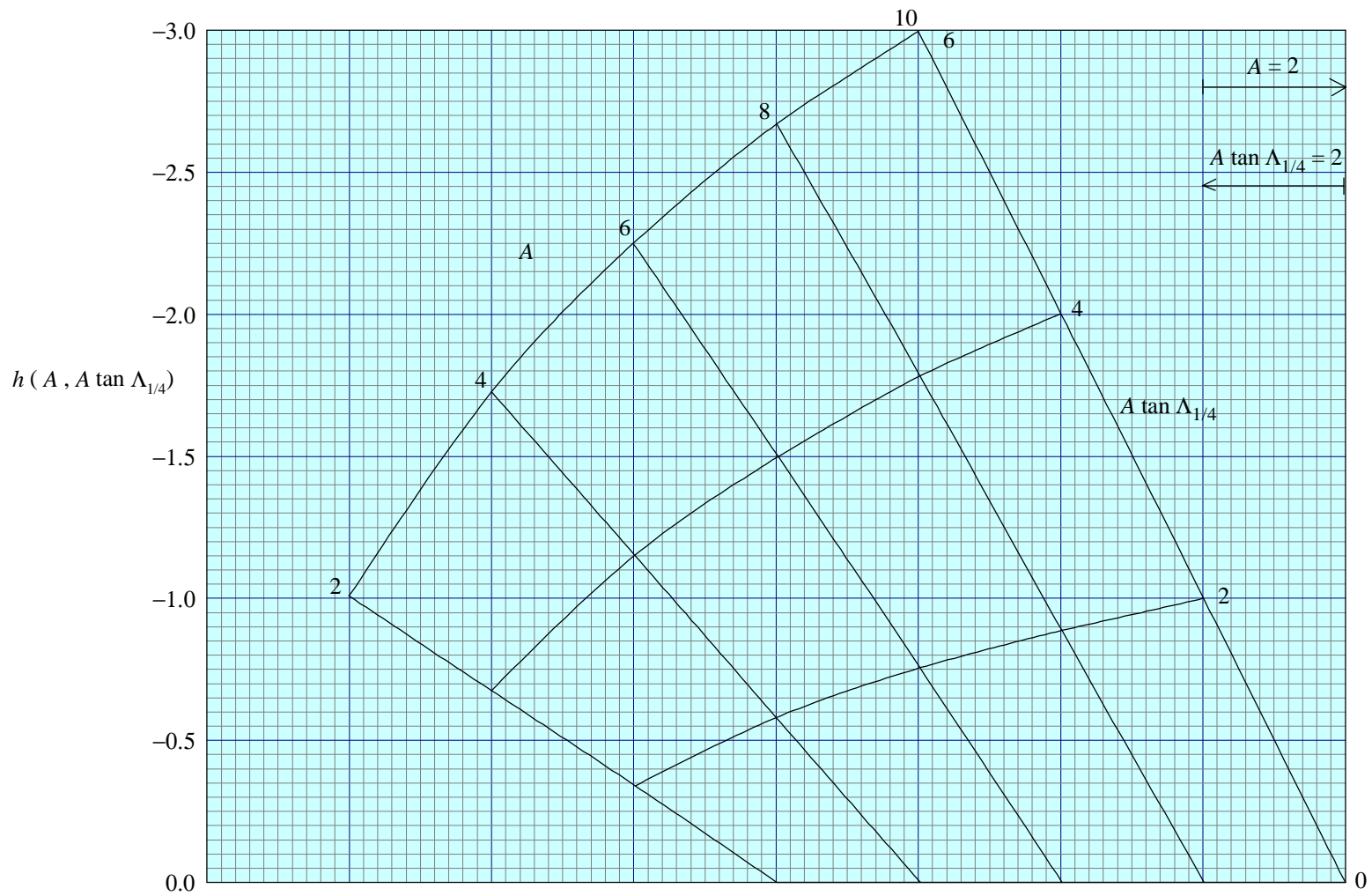


FIGURE 3

## APPENDIX A

### PROGRAM FOR CALCULATING WING PITCHING MOMENT AT ZERO LIFT AT SUBCRITICAL MACH NUMBERS

Every reasonable effort has been made to ensure that the program performs the intended calculations satisfactorily. However, in common with all providers of software, ESDU International cannot guarantee the suitability or fitness of the program for any particular purpose and no liability for any loss occasioned by any person as a direct or indirect result of use of the program, whether arising from negligence or otherwise, can be accepted. In no event shall ESDU International or any individuals associated with the development of the program be liable for any damage, including loss of profit or consequential loss, arising out of or in connection with the program.

#### A1. INTRODUCTION

A computer program, called ESDUpac A8701, for the method of the Item has been written by the Computer Products Group of ESDU International.

The program has been written in “STRICT” Microsoft FORTRAN 77 for use on machines using PC/MS DOS. A diskette containing files for the source code and some worked examples, together with an information file is provided in the Aerodynamics Software Volume. Guidance on copying, compilation and running the program is given in the “Introduction to ESDUpacs” in that volume. However, if any difficulty is experienced in using the program please contact ESDU International and we will do all we can to assist in overcoming the problem.

Section A2 describes the data required for the input file and Section A3. gives a number of examples of input and output using the program, including those in Section 6.

#### A2. INPUT

The following is a complete list of the input file data required. However, not all the data are required in every case, as explained later, for the various combinations of camber and twist.

Variable Name	Notation in Item	Units	Definition
A	$A$	–	Aspect ratio.
SB25	$\Lambda_{1/4}$	degree	Sweepback of 1/4-chord line.
SB50	$\Lambda_{1/2}$	degree	Sweepback of mid-chord line.
LAMBDA	$\lambda$	–	Taper ratio.
M	$M$	–	Free-stream Mach number.
ICAM	–	–	Pointer to indicate camber line constant or varying across span (see NOTE 1).
ITWIST	–	–	Pointer to indicate whether or not the wing has geometric twist (see NOTE 2).
CINF	$(C_{m0i})_{\infty th}$	–	Aerofoil theoretical pitching moment coefficient at zero-lift in low-speed flow (from Item No. 72024).
ALF	$(\alpha_{0ir})_{\infty}$	degree	Zero-lift angle for wing root section in low-speed flow (from Item No. 87031).

Variable Name	Notation in Item	Units	Definition
ALF20	$(\alpha_{0i, 0.2})_{\infty}$	degree	Zero-lift angle for section at $\eta = 0.2$ in low-speed flow (from Item No. 87031).
ALF80	$(\alpha_{0i, 0.8})_{\infty}$	degree	Zero-lift angle for section at $\eta = 0.8$ in low-speed flow (from Item No. 87031).
C20	$[(C_{m0i})_{\infty th}]_{0.2}$	–	Theoretical pitching moment coefficient at zero-lift in low-speed flow for section at $\eta = 0.2$ (from Item No. 72024).
C80	$[(C_{m0i})_{\infty th}]_{0.8}$	–	Theoretical pitching moment coefficient at zero-lift in low-speed flow for section at $\eta = 0.8$ (from Item No. 72024).
D20	$\delta_{0.2}$	degree	Geometric twist at $\eta = 0.2$ .
D80	$\delta_{0.8}$	degree	Geometric twist at $\eta = 0.8$ .

**NOTE:**

- (1) For camber line constant across the span, ICAM = 1. For camber line varying across the span, ICAM = 0.
- (2) For spanwise geometric twist, ITWIST = 1. For no geometric twist, ITWIST = 0.

Required input for various combinations of camber and twist:-

ICAM = 1 ITWIST = 0	ICAM = 1 ITWIST = 1	ICAM = 0 ITWIST = 0	ICAM = 0 ITWIST = 1
A	A	A	A
SB25	SB25	SB25	SB25
SB50	SB50	SB50	SB50
LAMBDA	LAMBDA	LAMBDA	LAMBDA
M	M	M	M
1	1	0	0
0	1	0	1
CINF	CINF	ALF	ALF
	D20	ALF20	ALF20
	D80	ALF80	ALF80
		C20	C20
		C80	C80
			D20
			D80

## A3. EXAMPLES OF INPUT AND OUTPUT

Sections A3.1 and A3.2 concern Examples 1 and 2 given in Section 6 of the Item. Additional examples are given in Sections A3.3 to A3.5 to illustrate, firstly, the other two possible combinations of camber and twist for the wing planform and Mach number used in Examples 1 and 2, and secondly a case of forward sweep.

### A3.1 Example 1

This is an example with ICAM = 1, ITWIST = 1.

#### *Input*

```
7
25
21.3
0.3
0.8
1
1
-0.0589
-1
-4
```

#### *Output*

```
-----
ESDU International plc
Program A8701
```

```
ESDUpac Number: A8701
ESDUpac Title: WING PITCHING MOMENT AT ZERO LIFT AT SUBCRITICAL
MACH NUMBERS
Data Item Number: 87001
Data Item Title: WING PITCHING MOMENT AT ZERO LIFT AT SUBCRITICAL
MACH NUMBERS
ESDUpac Version: 1.1 JULY 1991 -- Data Item Amendment B
(See Data Item for full input/output specification and interpretation)
-----
```

```
ASPECT RATIO = 7.000
SWEEPBACK OF 1/4-CHORD LINE = 25.00
SWEEPBACK OF MID-CHORD LINE = 21.30
TAPER RATIO = .3000
FREE-STREAM MACH NUMBER = .8000
```

```
RESULTS FOR CAMBER LINE CONSTANT ACROSS SPAN
WITH SPANWISE GEOMETRIC TWIST
```

```
(Cmoi)infTH = -.5890E-01
(Cmoi)l = -.4472E-01
(Cmo)l = -.7137E-01

DELTA0.2 = -1.000
DELTA0.8 = -4.000
DELTA'et = -5.000
```

```

(Cmoi)2          = .2388E-01
(Cmo)2          = .2859E-01

Cmo             = -.4278E-01

```

### A3.2 Example 2

This is an example with ICAM = 0, ITWIST = 1.

#### *Input*

```

7
25
21.3
0.3
0.8
0
1
0
-0.336
-1.344
-0.0118
-0.0471
-1
-4

```

#### *Output*

```

-----
ESDU International plc
Program  A8701

```

```

ESDUpac Number:  A8701
ESDUpac Title:   WING PITCHING MOMENT AT ZERO LIFT AT SUBCRITICAL
                  MACH NUMBERS
Data Item Number: 87001
Data Item Title:  WING PITCHING MOMENT AT ZERO LIFT AT SUBCRITICAL
                  MACH NUMBERS
ESDUpac Version: 1.1 JULY 1991 -- Data Item Amendment B
(See Data Item for full input/output specification and interpretation)
-----

```

```

ASPECT RATIO          = 7.000
SWEEPBACK OF 1/4-CHORD LINE = 25.00
SWEEPBACK OF MID-CHORD LINE = 21.30
TAPER RATIO           = .3000
FREE-STREAM MACH NUMBER = .8000

```

RESULTS FOR CAMBER LINE VARYING ACROSS SPAN  
WITH SPANWISE GEOMETRIC TWIST

```

(ALPHAoir)inf          = .0000
(ALPHAoi,0.2)inf       = -.3360
(Cmoi)infTH]0.2        = -.1180E-01
(ALPHAoi,0.8)inf       = -1.344
[(Cmoi)infTH]0.8       = -.4710E-01

```

```

(Cmoi)1          = -.1548E-01
(Cmo)1           = -.2471E-01

DELTAe0.2       = -.6640
DELTAe0.8       = -2.656
DELTA'et        = -3.320

(Cmoi)2         = .1586E-01
(Cmo)2          = .1899E-01

Cmo             = -.5724E-02

```

### A3.3 Example 3

This is an example with ICAM = 1, ITWIST = 0.

#### *Input*

```

7
25
21.3
0.3
0.8
1
0
-0.0589

```

#### *Output*

```

-----
ESDU International plc
Program A8701

```

```

ESDUpac Number:   A8701
ESDUpac Title:    WING PITCHING MOMENT AT ZERO LIFT AT SUBCRITICAL
                  MACH NUMBERS
Data Item Number: 87001
Data Item Title:  WING PITCHING MOMENT AT ZERO LIFT AT SUBCRITICAL
                  MACH NUMBERS
ESDUpac Version:  1.1 JULY 1991 -- Data Item Amendment B
(See Data Item for full input/output specification and interpretation)

```

```

-----
ASPECT RATIO              = 7.000
SWEEPBACK OF 1/4-CHORD LINE = 25.00
SWEEPBACK OF MID-CHORD LINE = 21.30
TAPER RATIO               = .3000
FREE-STREAM MACH NUMBER   = .8000

```

```

RESULTS FOR CAMBER LINE CONSTANT ACROSS SPAN
WITH NO SPANWISE GEOMETRIC TWIST

```

```

(Cmoi)infTH          = -.5890E-01
(Cmoi)1              = -.4472E-01
(Cmo)1               = -.7137E-01

(Cmoi)2              = .0000

Cmo                  = -.7137E-01

```

### A3.4 Example 4

This is an example with ICAM = 0, ITWIST = 0.

#### *Input*

```
7
25
21.3
0.3
0.8
0
0
0
-0.336
-1.344
-0.0118
-0.0471
```

#### *Output*

```
-----
ESDU International plc
Program A8701
```

```
ESDUpac Number:   A8701
ESDUpac Title:    WING PITCHING MOMENT AT ZERO LIFT AT SUBCRITICAL
                  MACH NUMBERS
Data Item Number: 87001
Data Item Title:  WING PITCHING MOMENT AT ZERO LIFT AT SUBCRITICAL
                  MACH NUMBERS
ESDUpac Version:  1.1 JULY 1991 -- Data Item Amendment B
(See Data Item for full input/output specification and interpretation)
-----
```

```
ASPECT RATIO                = 7.000
SWEEPBACK OF 1/4-CHORD LINE = 25.00
SWEEPBACK OF MID-CHORD LINE = 21.30
TAPER RATIO                 = .3000
FREE-STREAM MACH NUMBER     = .8000
```

```
RESULTS FOR CAMBER LINE VARYING ACROSS SPAN
WITH NO SPANWISE GEOMETRIC TWIST
```

```
(ALPHAair)inf                = .0000
(ALPHAoi,0.2)inf            = -.3360
(Cmoi)inf[TH]0.2          = -.1180E-01
(ALPHAoi,0.8)inf            = -1.344
[(Cmoi)inf[TH]0.8          = -.4710E-01

(Cmoi)1                    = -.1548E-01
(Cmo)1                     = -.2471E-01

DELTAe0.2                  = .3360
DELTAe0.8                  = 1.344
DELTA'et                   = 1.680
```

```
(Cmoi)2          = -.8025E-02
(Cmo)2           = -.9607E-02

Cmo              = -.3432E-01
```

### A3.5 Example 5

This is an example for a wing with forward sweep and ICAM = 0, ITWIST = 1.

#### *Input*

```
12
-30
-30
1
0.8
0
1
0
-0.386
-1.544
-0.0118
-0.0471
-1
-4
```

#### *Output*

```
-----
ESDU International plc
Program  A8701

ESDUpac Number:   A8701
ESDUpac Title:    WING PITCHING MOMENT AT ZERO LIFT AT SUBCRITICAL
                  MACH NUMBERS
Data Item Number: 87001
Data Item Title:  WING PITCHING MOMENT AT ZERO LIFT AT SUBCRITICAL
                  MACH NUMBERS
ESDUpac Version:  1.1 JULY 1991 -- Data Item Amendment B
(See Data Item for full input/output specification and interpretation)
-----
```

```
WARNING! ASPECT RATIO IS NOT IN THE RANGE 2 TO 10
SEE SECTION 4 OF DATA ITEM NO.87001
```

```
WARNING! FOR FORWARD SWEPT WINGS SEE SECTION 4 OF DATA ITEM NO.87001
```

```
ASPECT RATIO          = 12.00
SWEEPBACK OF 1/4-CHORD LINE = -30.00
SWEEPBACK OF MID-CHORD LINE = -30.00
TAPER RATIO           = 1.000
FREE-STREAM MACH NUMBER = .8000
```

```
RESULTS FOR CAMBER LINE VARYING ACROSS SPAN
WITH SPANWISE GEOMETRIC TWIST
```

---

(ALPHAOir)inf	= .0000
(ALPHAOi,0.2)inf	= -.3860
(Cmoi)infTH]0.2	= -.1180E-01
(ALPHAOi,0.8)inf	= -1.544
[(Cmoi)infTH]0.8	= -.4710E-01
(Cmoi)1	= -.2214E-01
(Cmo)1	= -.3594E-01
DELTAe0.2	= -.6140
DELTAe0.8	= -2.456
DELTA'et	= -3.070
(Cmoi)2	= -.4931E-01
(Cmo)2	= -.6307E-01
Cmo	= -.9900E-01

## THE PREPARATION OF THIS DATA ITEM

The work on this particular Item, which supersedes Item No. Aero W.08.03.01, was monitored and guided by the Aerodynamics Committee which first met in 1942 and now has the following membership:

Chairman	
Mr H.C. Garner	– Independent
Vice-Chairman	
Mr P.K. Jones	– British Aerospace plc, Civil Aircraft Div., Woodford
Members	
Mr E.A. Boyd	– Cranfield Institute of Technology
Mr K. Burgin	– Southampton University
Mr A. Condaminas	– Aérospatiale, Toulouse, France
Dr T.J. Cummings	– Short Brothers plc
Mr W.S. Chen*	– Northrop Corporation, Hawthorne, Calif., USA
Mr J.R.J. Dovey	– Independent
Dr J.W. Flower	– Bristol University
Mr A. Hipp	– British Aerospace plc, Army Weapons Div., Stevenage
Mr R. Jordan	– Aircraft Research Association
Mr J. Kloos*	– Saab-Scania, Linköping, Sweden
Mr J.R.C. Pedersen	– Independent
Mr I.H. Rettie*	– Boeing Aerospace Company, Seattle, Wash., USA
Mr R. Sanderson	– Messerschmitt-Bölkow-Blohm GmbH, Hamburg, W. Germany
Mr A.E. Sewell*	– McDonnell Douglas, Long Beach, Calif., USA
Mr M.R. Smith	– British Aerospace plc, Military Aircraft Div., Weybridge
Mr F.W. Stanhope	– Rolls-Royce plc, Derby.

\* Corresponding Member

The technical work involved in the assessment of the available information and the construction and subsequent development of the Data Item was undertaken by

Mr P. D. Chappell – Head of the Aircraft Aerodynamics Group.